

Supplementary Materials

Naphthalimide-piperazine derivatives as multifunctional “on” and “off” fluorescent switches for pH, Hg²⁺ and Cu²⁺ ions

Kristina Pršir ¹, Mislav Matić ¹, Marlena Grbić ¹, Gerhard J. Mohr ², Svjetlana Krištafor ¹ and Ivana Murković Steinberg ^{1,*}

¹ Department of General and Inorganic Chemistry, Faculty of Chemical Engineering and Technology, University of Zagreb, Marulićev trg 19, 10000 Zagreb, Croatia; kbobanov@fkit.hr (K.P.); mmatic@fkit.hr (M.M); marlena.grbic@iqvia.com (M.G.); prekupec@fkit.hr (S.K.)

² Joanneum Research Forschungsgesellschaft mbH – Materials, Franz-Pichler-Straße 30, Weiz A-8160, Austria; gerhard.mohr@joanneum.at (G.J.M.)

* Correspondence: imurkov@fkit.hr (I.M.S.)

Figure S1. Absorbance spectra of: a) **NI-1** and c) **NI-2** in a buffer/methanol mixture (2:1) at different pH; plot of absorbance ratio at 388 nm and 410 nm vs. pH for: b) **NI-1** and d) **NI-2**.

Figure S2. a) Fluorescence spectra of **NI-2** in buffer methanol mixture (2:1) at different pH; b) fluorescence intensity at 525 nm vs. pH.

Figure S3. **NI-1** in the presence of metal ions (from left: blank, Zn²⁺, Fe²⁺, Fe³⁺, Cu²⁺, Al³⁺, Hg²⁺, Pb²⁺, Co²⁺, Ni²⁺, Ag⁺, Mn²⁺, Ba²⁺, Cd²⁺, Mg²⁺, Ca²⁺) c (metal ion) = 3.0×10^{-5} M.

Figure S4. UV-Vis spectra of **NI-1** solution upon the addition of 20 equiv. of a) Hg(II) and b) Cu(II) ions.

Figure S5. Changes in the emission spectra of **NI-1** upon gradual addition of Cu²⁺ and EDTA.

Figure S6. Changes in the emission spectra of **NI-1** upon gradual addition of Hg²⁺ and EDTA.

Figure S7. Benesi-Hildebrand's plot in linear range for **NI-1** binding with a) Cu²⁺ b) Hg²⁺.

Figure S8. Dependence of fluorescence intensity of **NI-1** (5.00×10^{-7} M) in MeOH / buffer pH 5.5 (v / v, 1/2) at 523 nm on the ion concentration in the linear range of dependence for a) Cu^{2+} b) Hg^{2+} ion.

Figure S9. Stern-Volmer plot of the ratio of the fluorescence intensities (F_0/F) of **NI-1** against the increasing concentration of a) Cu^{2+} and b) Hg^{2+} ions in linear range.

Figure S10. UV-Vis spectra of **NI-2** upon the addition of Hg(II) ions.

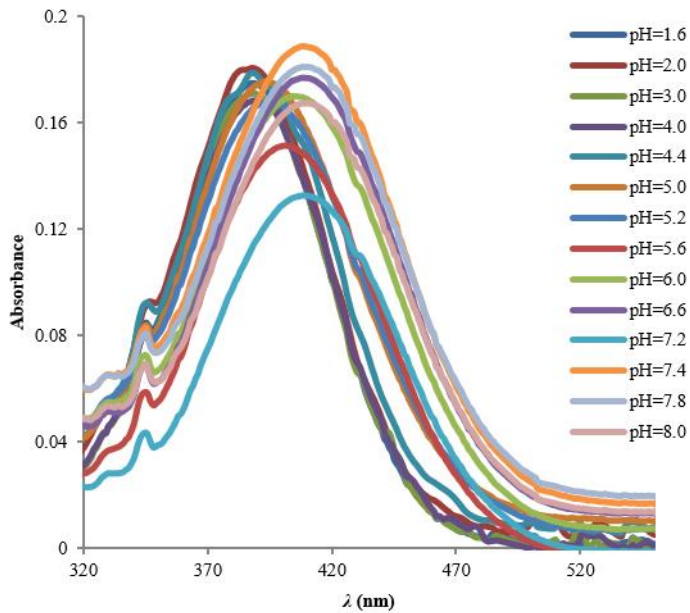
Figure S11. Job's plot fluorescence intensity at 525 nm on the molar content of **NI-2** in presence of Hg^{2+} ions at a total concentration of 5.00×10^{-6} M. The extrapolated directions of intensity dependence on the molar fraction of **NI-2** are presented.

Figure S12. Benesi-Hildebrand's plot in linear range for **NI-2** binding with Hg^{2+} .

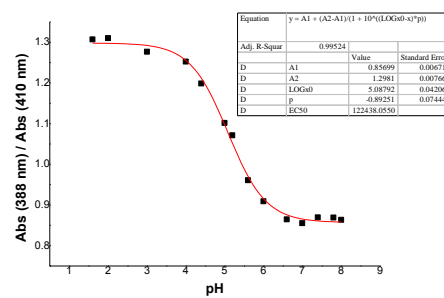
Figure S13. Dependence of fluorescence intensity of **NI-2** (6.53×10^{-6} M) in MeOH / buffer 5.5 (v/v, 1/2) at 525 nm on the ion concentration in the linear range of dependence for Hg^{2+} ion.

Figure S14. Reversibility test for **NI-2** and Hg(II) binding.

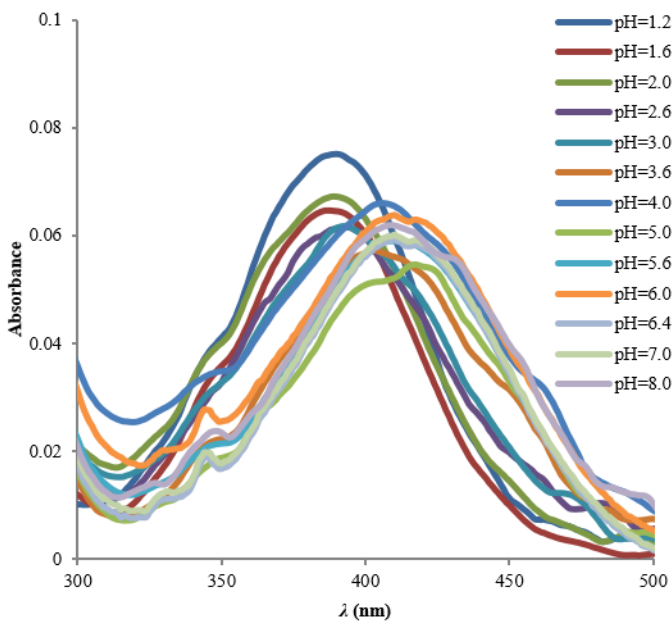
a)



b)



c)



d)

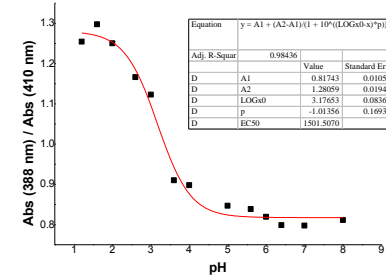


Figure S1. Absorbance spectra of: a) **NI-1** and c) **NI-2** in a buffer/methanol mixture (2:1) at different pH; plot of absorbance ratio at 388 nm and 410 nm vs. pH for: b) **NI-1** and d) **NI-2**. The spectra of compounds **NI-1** and **NI-2** were recorded in MeOH/buffer (1:2) at compound concentrations 6.56×10^{-5} M and 6.54×10^{-5} M, respectively.

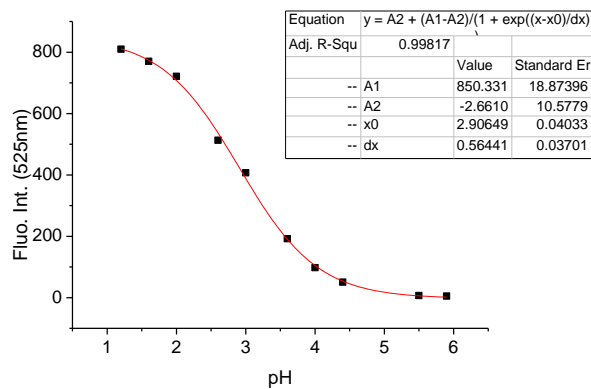
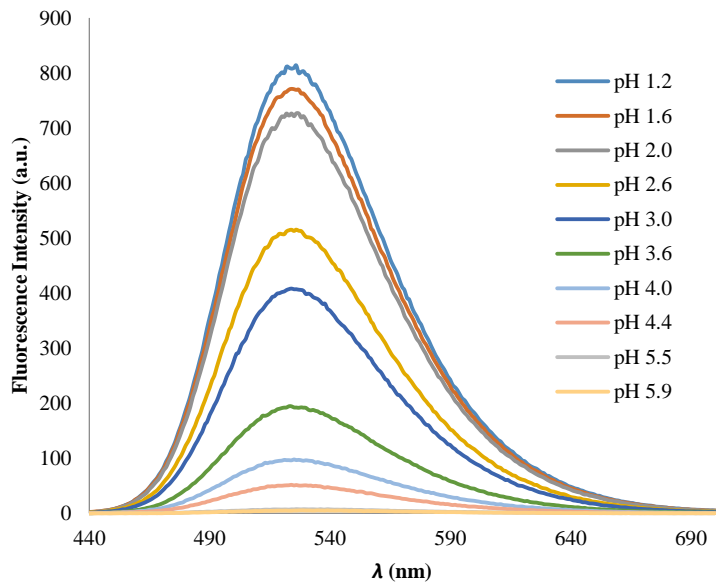


Figure S2. a) Fluorescence spectra of **NI-2** in buffer methanol mixture (2:1) at different pH; b) fluorescence intensity at 525 nm vs. pH.

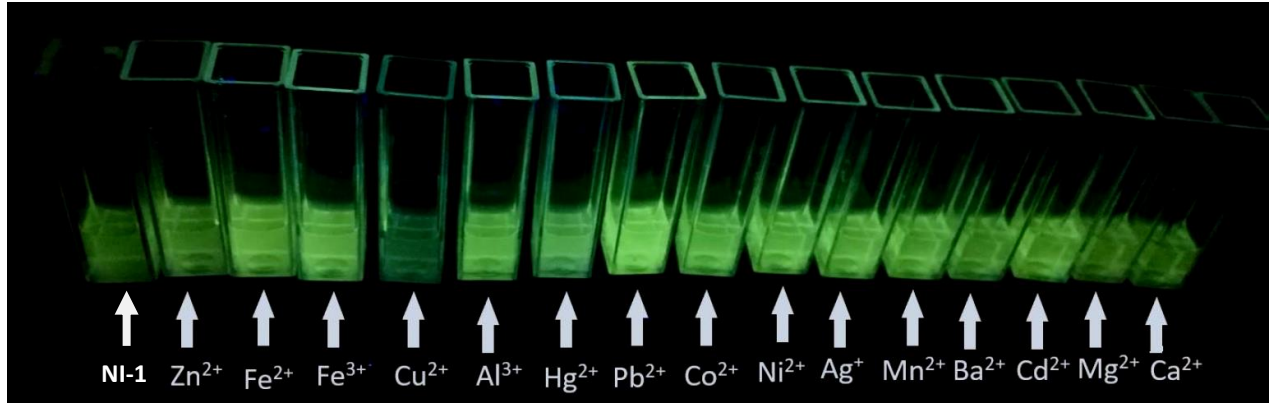


Figure S3. NI-1 in the presence of metal ions (from left: blank, Zn^{2+} , Fe^{2+} , Fe^{3+} , Cu^{2+} , Al^{3+} , Hg^{2+} , Pb^{2+} , Co^{2+} , Ni^{2+} , Ag^+ , Mn^{2+} , Ba^{2+} , Cd^{2+} , Mg^{2+} , Ca^{2+}) c (metal ion) = 3.0×10^{-5} M.

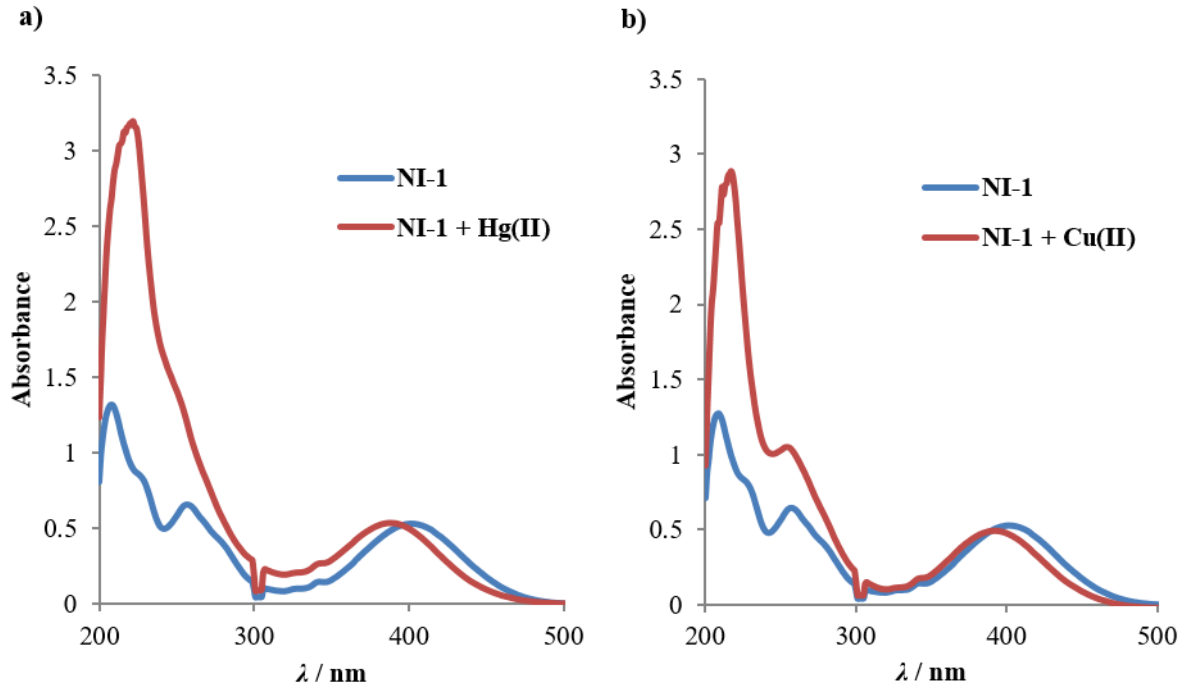


Figure S4. UV-Vis spectra of NI-1 solution upon the addition of 20 equiv. of a) Hg(II) and b) Cu(II) ions.

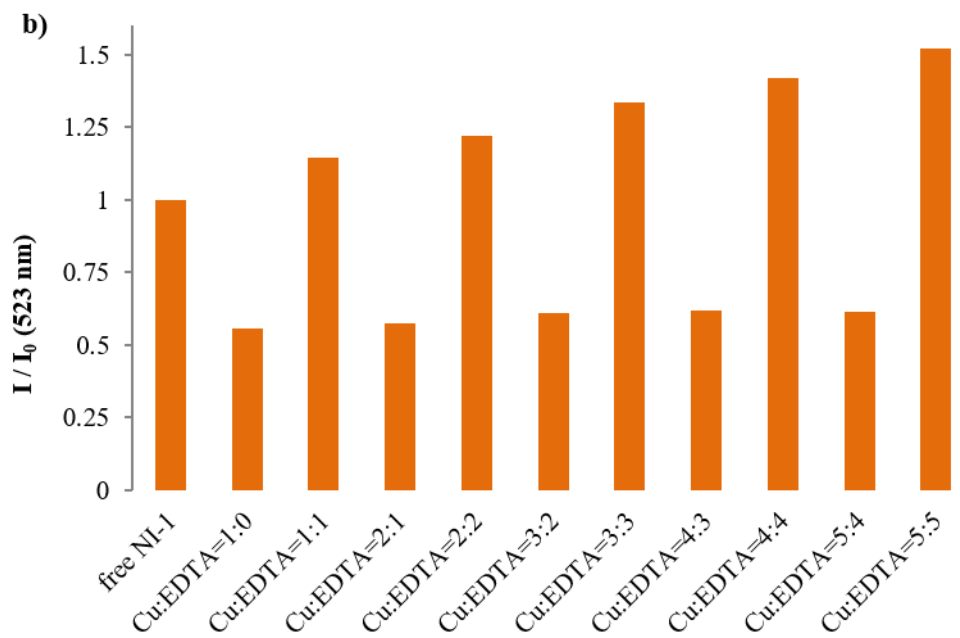
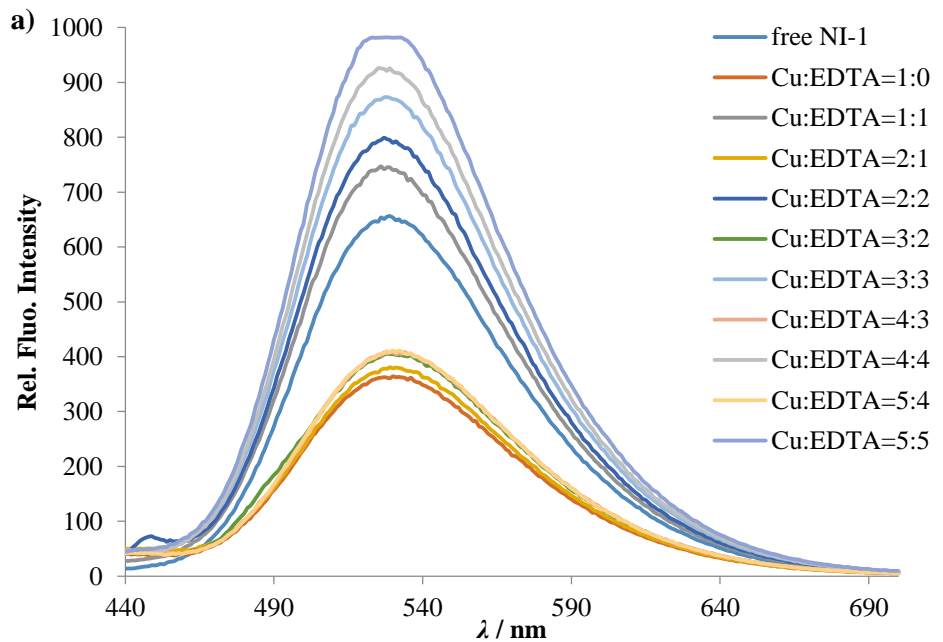


Figure S5. Changes in the emission spectra of **NI-1** upon gradual addition of Cu^{2+} and EDTA.

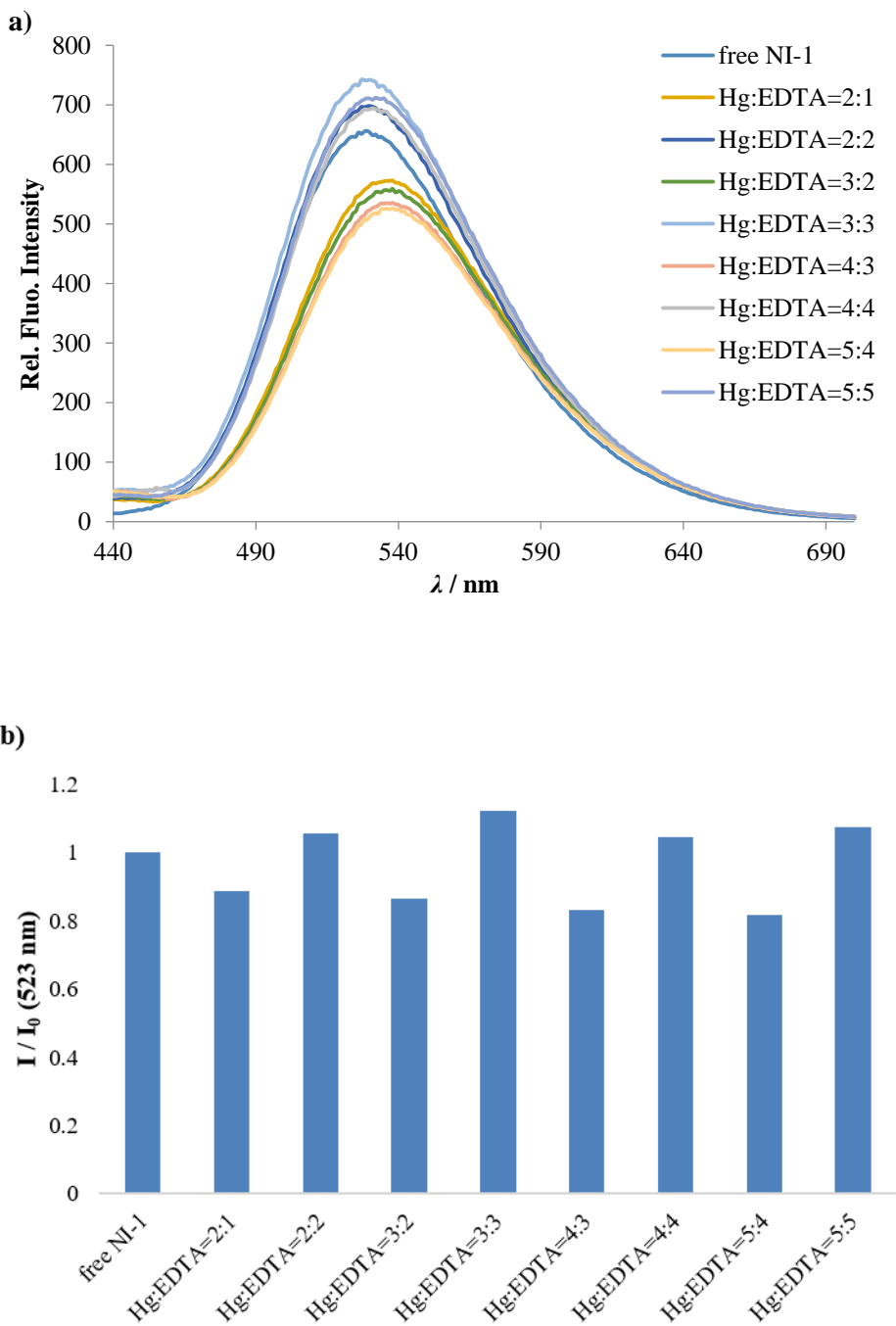


Figure S6. Changes in the emission spectra of **NI-1** upon gradual addition of Hg^{2+} and EDTA.

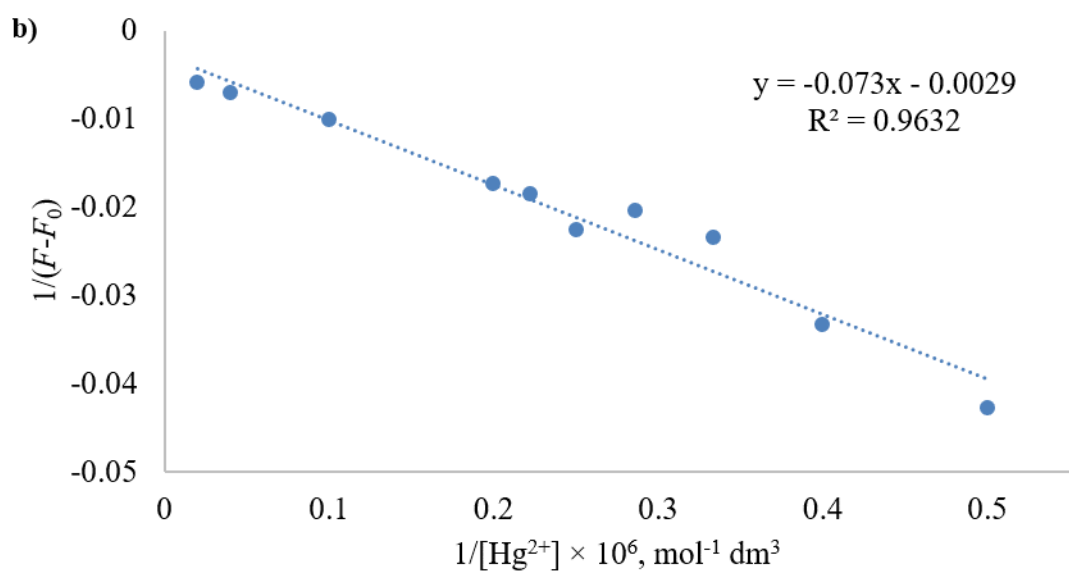
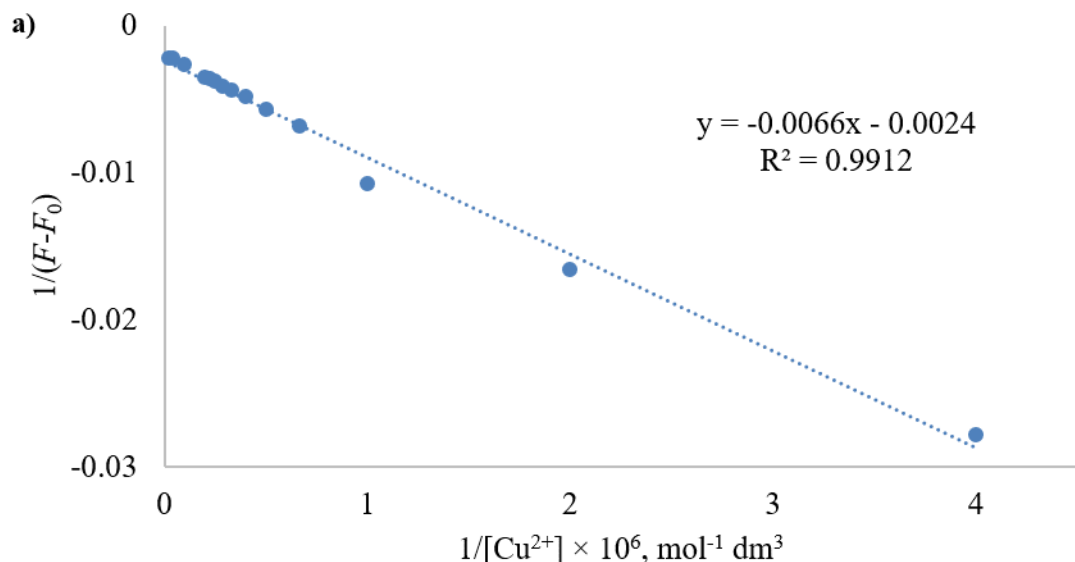


Figure S7. Benesi-Hildebrand's plot in linear range for **NI-1** binding with a) Cu^{2+} b) Hg^{2+} .

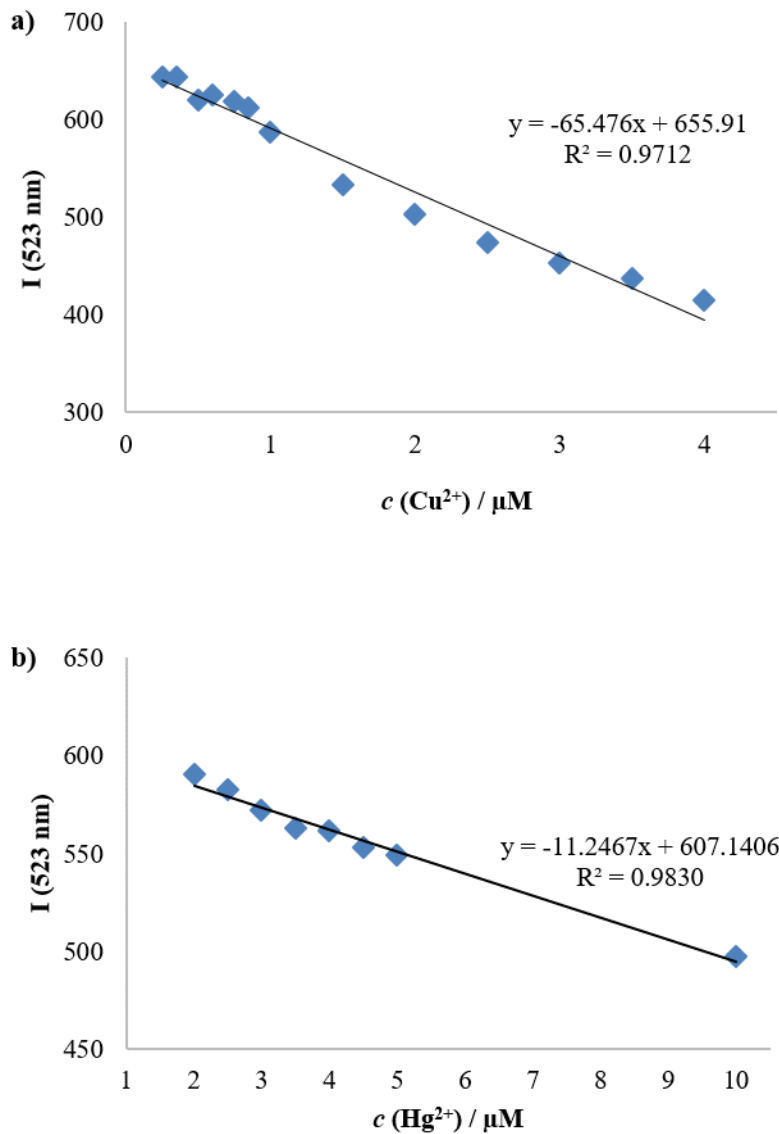


Figure S8. Dependence of fluorescence intensity of **NI-1** (5.00×10^{-7} M) in MeOH / buffer pH 5.5 (v / v, 1/2) at 523 nm on the ion concentration in the linear range of dependence for a) Cu²⁺ b) Hg²⁺ ion.

Stern-Volmer's equation for **NI-1** was derived using:

$$\frac{F_0}{F} = 1 + K_{sv}[Q]$$

where F_0 - initial fluorescence intensity, F – fluorescence intensity in the presence of the analyte, $[Q]$ – concentration of fluorescence quencher (Cu^{2+} or Hg^{2+} ion), K_{sv} – Stern-Volmer constant.

The Stern-Volmer constant is equal to the slope in the linear range of the fluorescence intensity ratio of **NI-1** without metal ions and fluorescence intensity in the presence of ions at 523 nm as shown in Fig. S10. For Cu^{2+} ion the Stern-Volmer constant is 152570 M^{-1} , and for Hg^{2+} ion it is 23909 M^{-1} .

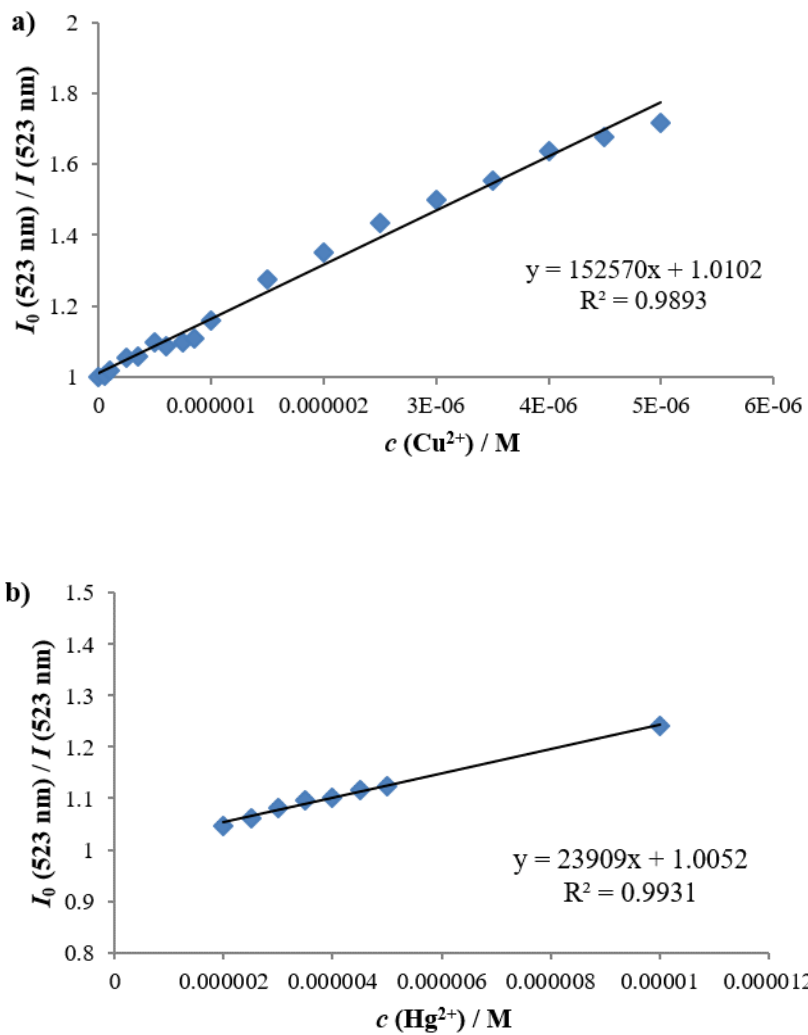


Figure S9. Stern-Volmer plot of the ratio of the fluorescence intensities (F_0/F) of **NI-1** against the increasing concentration of a) Cu^{2+} and b) Hg^{2+} ions in linear range.

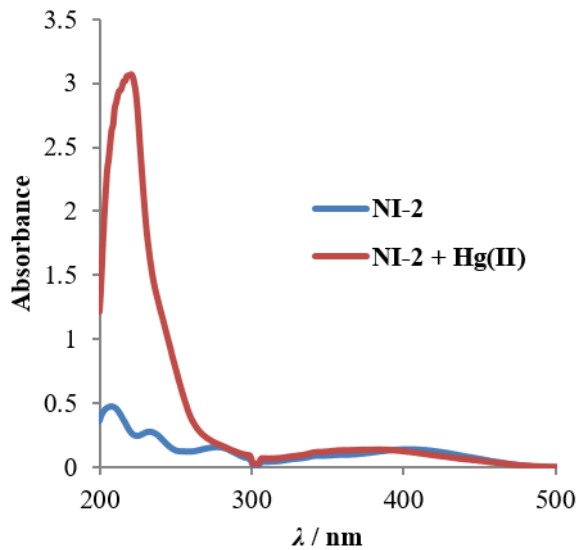


Figure S10. UV-Vis spectra of **NI-2** upon the addition of $\text{Hg}(\text{II})$ ions.

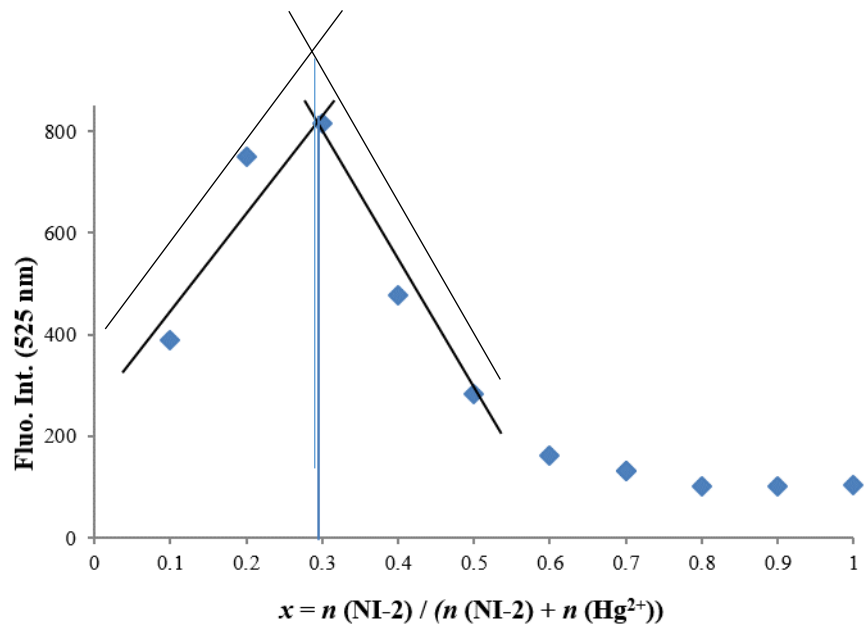


Figure S11. Job's plot fluorescence intensity at 525 nm on the molar content of **NI-2** in presence of Hg^{2+} ions at a total concentration of 5.00×10^{-6} M. The extrapolated directions of intensity dependence on the molar fraction of **NI-2** are presented.

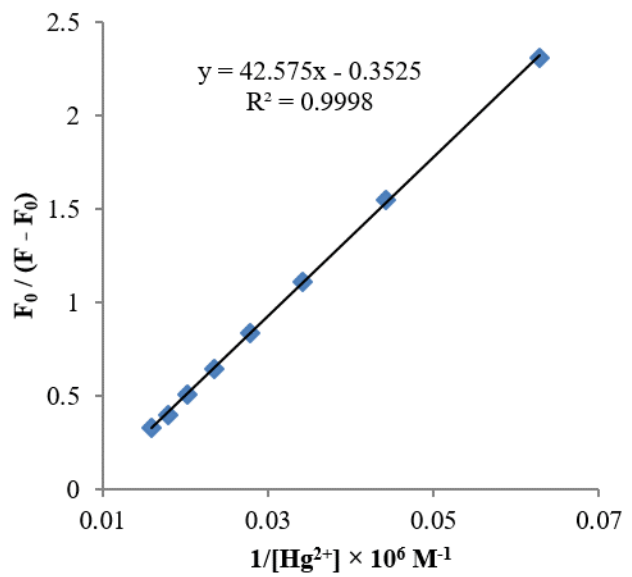


Figure S12. Benesi-Hildebrand's plot in linear range for NI-2 binding with Hg^{2+} .

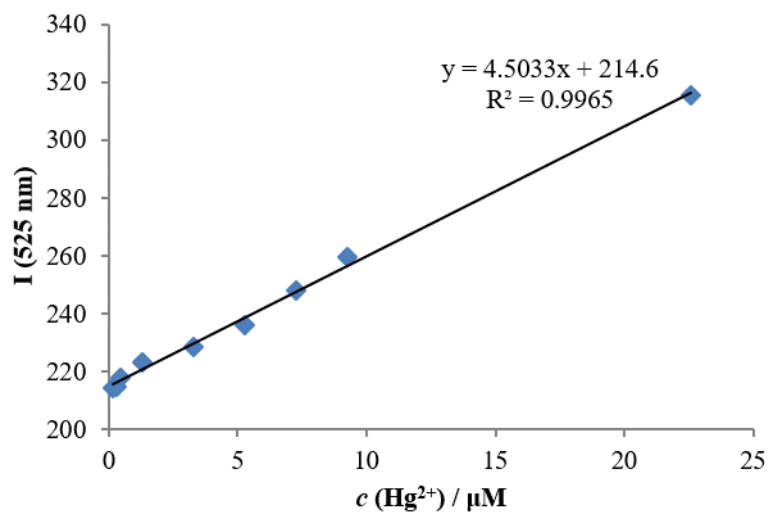


Figure S13. Dependence of fluorescence intensity of **NI-2** (6.53×10^{-6} M) in MeOH / buffer 5.5 (v/v, 1/2) at 525 nm on the ion concentration in the linear range of dependence for Hg^{2+} ion.

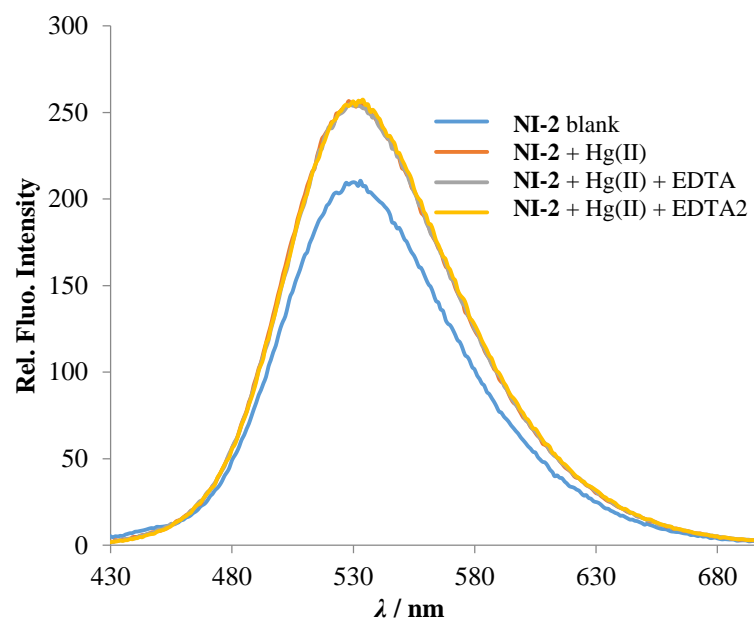


Figure S14. Reversibility test for **NI-2** and $\text{Hg}(\text{II})$ binding.